

# RSC Advances



This is an *Accepted Manuscript*, which has been through the Royal Society of Chemistry peer review process and has been accepted for publication.

*Accepted Manuscripts* are published online shortly after acceptance, before technical editing, formatting and proof reading. Using this free service, authors can make their results available to the community, in citable form, before we publish the edited article. This *Accepted Manuscript* will be replaced by the edited, formatted and paginated article as soon as this is available.

You can find more information about *Accepted Manuscripts* in the [Information for Authors](#).

Please note that technical editing may introduce minor changes to the text and/or graphics, which may alter content. The journal's standard [Terms & Conditions](#) and the [Ethical guidelines](#) still apply. In no event shall the Royal Society of Chemistry be held responsible for any errors or omissions in this *Accepted Manuscript* or any consequences arising from the use of any information it contains.

1           **Shell cross-linked polyethylenimine-modified micelles for temperature-**  
2                           **triggered drug release and gene delivery**

3  
4                           Su-Yeon Lee<sup>1,3</sup>, Seong-Jun Choi<sup>1,2</sup>, Seog-Jin Seo<sup>1,2,\*</sup>, Hae-Won Kim<sup>1,2,3,\*</sup>

5  
6           <sup>1</sup>Institute of Tissue Regeneration Engineering (ITREN), Dankook University, Cheonan, 330–714,  
7           Republic of Korea

8           <sup>2</sup>Department of Nanobiomedical Science & BK21 PLUS NBM Global Research Center for  
9           Regenerative Medicine, Dankook University, Cheonan, 330–714, Republic of Korea

10          <sup>3</sup>Department of Biomaterials Science, School of Dentistry, Dankook University, Cheonan, 330–714,  
11          Republic of Korea

12  
13  

---

14          \* **Corresponding authors: Seog-Jin Seo and Hae-Won Kim**

15          - *E-mail* [seosj203@dankook.ac.kr](mailto:seosj203@dankook.ac.kr); [kimhw@dku.edu](mailto:kimhw@dku.edu) ;

16          - *Tel:* + 82 41 550 3081; *Fax:* +82 41 550 3085;

17          - *Mailing address:* Institute of Tissue Regeneration Engineering (ITREN), Dankook University, Cheonan, 330–714,  
18          Republic of Korea

19

20

21 **Abstract**

22 Stimuli-responsiveness is an important characteristic of nanocarriers that can deliver therapeutic  
23 molecules in a controlled and on-demand manner. In particular, temperature-responsive micelles have  
24 recently gained increasing attention for use in diverse therapeutic areas, including hyperthermia  
25 therapy. Herein, we developed novel shell cross-linked Pluronic F127 (PF127) polymers with  
26 branched polyethylenimine (PEI), called FPEI, for temperature-triggered drug delivery and gene  
27 transfection. The successful synthesis of FPEI copolymers was confirmed by Fourier-Transform  
28 Infrared spectroscopy, with the weight percent of PEI in the FPEI copolymers being 7.5%. The critical  
29 micelle concentration of FPEI and PF127 copolymers was shown to be 0.013 and 0.03 mg/ml at room  
30 temperature, respectively. When Nile Red (NR), used as a hydrophobic model drug, was loaded into  
31 FPEI copolymers, the appropriate concentration of NR was 3 and 5  $\mu\text{g/ml}$  in 5 and 10 mg/ml of FPEI,  
32 respectively. Interestingly, the loading capacity of FPEI increased with an increase in the micelle  
33 concentration. As temperature increased, the NR release from the micelle increased, while the micelle  
34 radii of FPEI, NR-loaded FPEI, and NR-loaded FPEI/DNA decreased. The DNA binding ability of FPEI  
35 copolymers increased with an increase in the N/P ratio. FPEI cytotoxicity in HeLa cells showed a  
36 similar tendency, when equivalent PEI amount in FPEI was treated. While further in-depth studies  
37 remain as to the in vitro and in vivo biological functions, the FPEI system demonstrated well  
38 temperature-triggered NR release into HeLa cells, along with sufficient transfection of plasmid green  
39 fluorescence protein, which suggested potential usefulness in temperature-responsive therapy.

40

41 **Keywords:** Temperature-responsive, Micelle, Multifunctional delivery, Transfection, Polyethylenimine,  
42 Pluronic F127, Gene delivery, Hyperthermia, Critical micelle concentration, Nile red

43

44

## 45 1. Introduction

46 The use of stimuli-triggered micelle delivery has received great attention in active targeting  
47 therapeutics, due to the unique properties of responding to specific stimuli and the protection of  
48 normal tissues or cells from the damaging effects of loaded biomolecules. The stimuli-triggered  
49 delivery system is designed to act by specified stimuli, such as temperature,<sup>1</sup> pH,<sup>2</sup> ionic strength,<sup>3</sup>  
50 magnet,<sup>4</sup> glutathione,<sup>5</sup> and light.<sup>6</sup> Among these stimuli, temperature has long been used as one of the  
51 most-effective signals due to the ease of manipulation and safety in medical applications, such as the  
52 hyperthermia treatment of solid tumors. For example, poly(N-isopropylacrylamide) (PNIPAAm) and  
53 Pluronics have been widely used for targeting therapeutics with local hyperthermia,<sup>7,8</sup> owing to the  
54 self-assembled micelle forming property in aqueous solutions.<sup>9,10</sup> Self-assembled micelles with  
55 nanoreservoir structure are able to encapsulate poorly water-soluble drugs in the hydrophobic core  
56 above the critical micelle concentration (CMC), leading to improved water solubility and efficiency of  
57 the release of therapeutic drugs. However, micelles composed of PNIPAAm or Pluronics can  
58 dissociate into polymeric units at low concentrations, below the CMC, upon dilution by body fluids  
59 during blood circulation, consequently losing their drug-loading capacity.<sup>11</sup> In addition, the nonionic  
60 nature of these polymers results in hardly forming gene complexes or facilitating cellular uptake.<sup>12</sup>  
61 Recently, one challenging approach to crosslinking the micellar shell to cationic polymers has been  
62 suggested not only to avoid micellar dissociation in the *in vivo* condition but also to facilitate gene  
63 complex formation,<sup>13-17</sup> which include chitosan,<sup>18</sup> poly-L-lysine<sup>19</sup> or polyethylenimine (PEI).<sup>20</sup> Of these,  
64 branched PEI containing primary, secondary, and tertiary amines is well-accepted as a non-viral gene  
65 carrier with high buffering capacity over a wide pH range. The unique structure and properties of PEI  
66 made possible to facilitate immediate formation of gene complexes, cellular uptake, and further  
67 endosomal escape.

68 In this work, Pluronic F127 (PF127)-crosslinked PEI (FPEI) nanoparticles were produced for  
69 temperature-triggered micellar release of drugs and gene transfection. The resultant FPEI  
70 nanoparticles were characterized with a focus on co-delivery of drugs and genes by thermal transition  
71 reaction.

## 72        **2. Materials and methods**

### 73                *2.1. Activation of PF127 with 4-nitrophenyl chloroformate (4-NPC)*

74 PF127 (MW 12500 Da, Sigma-Aldrich, USA) was activated with 4-NPC (Sigma-Aldrich, USA) as  
75 described by a previous report.<sup>21</sup> Briefly, a solution of PF127 (1 g) dissolved in 3 ml benzene was  
76 slowly added to a stirred solution of 4-NPC (0.05 g) in 3 ml benzene. After stirring for 24 h, the  
77 resultant was precipitated at least twice using an eight-fold excess of petroleum ether, and recovered  
78 by filtration by removal of the remaining solvent by evaporation under vacuum overnight. The  
79 substitution degree of *para*-nitrophenolate ions was determined in an alkaline solution (0.1 N NaOH)  
80 by spectrophotometry at 402 nm.

81

### 82                *2.2. Synthesis and characterization of FPEI*

83 FPEI was synthesized by a modified method as previously reported.<sup>21</sup> Briefly, activated PF127 (600  
84 mg) was added to 1.2 g of branched PEI (MW: 1,800 Da, Polysciences, Inc. USA) in 15 ml of 0.1 N  
85 NaOH. The reaction mixture was stirred for six hours at room temperature, and purified by a dialysis  
86 membrane with a molecular weight cut-off (MWCO) of 3,500 against deionized water for 3 days for  
87 freeze-drying. The synthesis of FPEI copolymers was confirmed by Fourier-Transform Infrared  
88 Spectrometry (FT-IR, Perkin Elmer, Spectrum BXII spectrometer, USA). The conjugated PEI content  
89 was calculated by a TNBS (2,4,6-trinitrobenzene sulfonic acid) assay.<sup>22</sup>

90

### 91                *2.3. Determination of critical micelle concentration (CMC)*

92 CMC was measured by a modified method as described by previous reports.<sup>23-25</sup> Briefly, a 0.5 mg/ml  
93 stock solution of Nile Red (NR) fluorophore (Sigma-Aldrich, USA) in acetone was prepared and stored  
94 at 4°C until use. NR is hardly water soluble, but exhibits strong fluorescence intensity even in tiny  
95 amounts. For the CMC measurement, FPEI in the aqueous solution was prepared in its

96 concentrations ranging from 0.0001 mg/ml to 1 mg/ml. To these polymer solutions, NR dissolved in  
97 acetone was added to become a final concentration of 5  $\mu\text{g/ml}$ . The resulting solutions were placed  
98 into a 96-well plate for a fluorescence measurement on a fluorescence plate reader (Spectramax M2,  
99 Molecular Devices, USA) with  $\lambda_{\text{ex}}=544$  nm and  $\lambda_{\text{em}}=612$  nm at room temperature. The CMC was  
100 determined as the intersection point on the two linear lines fitting the plots of the concentration-  
101 dependent section and the concentration-independent section. The hydrodynamic radii of FPEI, NR-  
102 loaded FPEI, and NR-loaded FPEI complexes with DNA at the concentrations exhibiting their  
103 morphological changes were measured on the basis of the principle of dynamic light scattering (DLS)  
104 using a Zetasizer (Malvern, Worcestershire, UK).<sup>26</sup>

105

#### 106 *2.4. NR loading efficiency and release*

107 FPEI solutions (1, 5, and 10 mg/ml) containing NR over the concentration range of 0.1-10  $\mu\text{g/ml}$  were  
108 prepared to measure the NR loading efficiency. The mixtures were incubated at 60°C for 1 h, cooled  
109 down to room temperature for 1 h to reach micellar equilibrium, and placed into a 96-well plate for  
110 measurement of fluorescence after filtration with a 0.45  $\mu\text{m}$  syringe filter. Loading efficiency was  
111 analyzed by measuring the fluorescence intensity of NR in the micelle solutions.

112 In order to assess temperature-dependent micelle release behaviors, the NR release study was  
113 performed using a dialysis method. In brief, 0.2 ml of 10 mg/ml of FPEI solutions loading 3  $\mu\text{g/ml}$  of  
114 NR fluorophore was placed into D-tube<sup>TM</sup> Dialyzer mini tubes with an MWCO of 6-8 kDa (EMD  
115 Millipore, Damstadt, Germany). Then, each group of samples was incubated at 25, 37, and 40°C. The  
116 released NR extract from the tube was then collected and replaced with fresh water (0.5 ml) after  
117 given periods of incubation time. The NR concentration in the released extract was determined by  
118 correspondence to standard curves of fluorescence for the molecules dissolved in 1 % acetone.  
119 Unreleased NR content in the dialysis tubes was measured to further analyze total NR amounts more  
120 precisely. The cumulative NR release (%) was calculated as the weight of the released NR to the  
121 weight of the total NR amounts fed.

122

123

#### 2.5. Gene complexes with FPEI copolymers

124 FPEI complexes with plasmid DNA were confirmed by agarose gel retardation. FPEI/DNA complex  
125 over an N/P ratio range up to 7.5 was loaded on a 1.5 % agarose gel containing 0.1 µg/ml of Red  
126 Safe (Intron, South Korea). The resulting DNA migration pattern was exhibited under UV irradiation.  
127 The surface charge of the FPEI/DNA complex over an N/P ratio range up to 100 was measured by the  
128 DLS method using a Zetasizer (Malvern, Worcestershire, UK).

129

130

#### 2.6. Cell culture for toxicity

131 For the *in vitro* cytotoxicity study of the FPEI copolymers, the human cervical cancer cell line (HeLa)  
132 was obtained from the American Type Culture Collection (ATCC, Rockville, MD, USA). All cells were  
133 maintained at 37 °C in an atmosphere of 5 % CO<sub>2</sub> in DMEM containing 10 % fetal bovine serum (FBS,  
134 Gibco, USA) and 1 % penicillin-streptomycin. The medium was regularly refreshed and the cells were  
135 passaged at confluence. The cells were plated in a 96-well plate at a density of 5 x 10<sup>3</sup> cells per well  
136 with 100 µl culture medium and cultured for 24 h. The sterilized PF127, FPEI, and PEI samples at  
137 various concentrations were added to each well of the plates, and incubated at 37 and 40°C for 1 h.  
138 Next, the plate that was incubated at 40°C was returned to an incubator at 37°C. At 48 h after  
139 treatment of the samples, the culture medium was replaced with fresh medium containing 10 % cell  
140 counting kit-8 solution (CCK-8, Dojindo, Japan), and incubated for another 4 h at 37°C. At the end of  
141 CCK-8 treatment, a 100 µl aliquot of each cell culture supernatant was collected and measured at 450  
142 nm using an iMark microplate reader (BioRad, USA).

143

144

#### 2.7. *In vitro* cell transfection and NR release

145 The cells were seeded into a 24-well plate at a density of 2.5 x 10<sup>4</sup> cells per well with 0.5 ml of culture

146 medium. Plasmid green fluorescence protein (GFP) (1  $\mu$ g) was added to NR (1 ng)-loaded FPEI  
147 micelles (0.04 mg), and incubated at room temperature for 30 min. Then, the complexes were added  
148 into each well and incubated at 37 and 40°C for 1 h. Next, the plate that was incubated at 40°C was  
149 returned to an incubator at 37°C. After 36 h of treatment of the samples, the culture medium was  
150 replaced with fresh medium and the cells were observed by an inverted fluorescence microscope (IX-  
151 71, Olympus, Japan).

152

### 153 **3. Results and discussion**

#### 154 *3.1. Synthesis of shell cross-linked FPEI micelles*

155 In this study, PEI was covalently conjugated with the end group of PF127 copolymers  
156 following 4-NPC activation, to produce a dual carrier that can facilitate drug loading and DNA complex  
157 formation with PEI. **Figure 1a** depicts the molecular structure of the synthesized FPEI, and a  
158 schematic diagram exhibiting the temperature-triggered drug release by the squeezing effect of the  
159 FPEI micelle complexes with the genes. The conjugation of PEI with PF127 was analyzed by FT-IR  
160 spectra over the range of 400-4000  $\text{cm}^{-1}$  for the PF127 and FPEI copolymers, as shown in **Figure 1b**.  
161 Distinctive amine (-NH-) stretching at 3450  $\text{cm}^{-1}$  and amine (-NH-) bending at 1630  $\text{cm}^{-1}$  detected  
162 were assigned to the amine groups of PEI in the FPEI spectrum, indicating covalent conjugation of  
163 PEI and PF127. The weight content of the total nitrogen molecules in the FPEI copolymer calculated  
164 by a TNBS assay was 7.5 %, possibly forming gene complexes and facilitating cellular uptake.

165

#### 166 *3.2. Self-assembled micelle formation of FPEI copolymers*

167 The CMC is a determinant parameter determining the relative thermodynamic stability of self-  
168 organized micelle aggregates in aqueous solutions. The polymeric CMC is determined by the  
169 fluorescence measurement of increasing polymer concentrations.<sup>27, 28</sup> Self-assembled micelles  
170 possessing the spherical core-shell structure are formed above the CMC, and fluorescence probes



171 can be used to determine the CMC.<sup>29</sup> The CMC of FPEI copolymers was found by a modified method  
172 using an NR fluorophore as a fluorescence probe.<sup>23</sup> **Figure 2a** shows the CMC measurement by the  
173 fluorescence intensity of the NR fluorophore, indexing arbitrary units as a function of copolymer  
174 concentrations. The micelle formation of FPEI and PF127 was achieved at concentrations above  
175 0.013 and 0.03 mg/ml, respectively. The CMC of FPEI micelles was approximately 2.3-fold lower than  
176 that of PF127, providing direct evidence for an increase in the colloidal stability upon shell cross-  
177 linking.<sup>30, 31</sup>

178 The hydrodynamic radii of free FPEI, NR-loaded FPEI, and NR-loaded FPEI complexes with  
179 DNA were measured by a DLS at increasing temperatures to examine the temperature-triggered  
180 behavior of the FPEI micelles (**Figure 2b**). Temperature-dependent decreases in particle diameter  
181 were monitored for the different types of samples with an increase in temperature. The diameter of the  
182 FPEI micelles was reduced from hundreds of nanometers at room temperature, to a few tens of  
183 nanometers above body temperature. Conversely, the size reduction degree of the NR-loaded FPEI  
184 micelles and their complexes with DNA was less than that of free FPEI micelles, owing to the  
185 presence of NR loaded in the micelle core. The temperature-dependent size change was attributed to  
186 the hydrophobic interaction by rigid PPO chains in the micelle core,<sup>23, 32</sup> while the hydrophobically  
187 condensed micelles may effectively release NR molecules.

188

### 189 *3.3. In vitro drug loading and release of thermosensitive FPEI micelles*

190 The loading efficiency of NR into FPEI micelles at the given concentrations (1, 5, and 10  
191 mg/ml) was investigated as a function of NR concentration, to understand the hydrophobic drug  
192 loading behavior of FPEI micelles. **Figure 3a** shows the NR loading efficiency, indicating the influence  
193 of FPEI concentration on how much payload of NR was possible. The loading efficiency was  
194 determined by fluorescence intensity quantification of the amount of NR which the FPEI micelles were  
195 capable of loading. The NR payload achievable without significant loss was shown to be appropriate  
196 at 3-5  $\mu\text{g/ml}$  after the purification process, i.e., the best aqueous stability was exhibited at the highly

197 achievable concentration of NR payload in the FPEI system. NR loading efficiencies of the FPEI  
198 micelles were dramatically improved with an increase in NR concentration (3-5  $\mu\text{g/ml}$ ), but were  
199 notably reduced above that concentration. This was possibly due to the precipitation of insoluble NR  
200 aggregates in aqueous media that might not be loaded into the FPEI micelles, indicating the loading  
201 capacity limit, which would decrease the room for drug entrapment.<sup>33-35</sup> From these results, it is  
202 important to note that the drug-loading capacity of FPEI micelles was significantly increased up to the  
203 extent of the optimal drug concentration, upon finding the appropriate drug payload. The results  
204 implied that drug-loading capacity was largely dependent on hydrophobic interaction with PPO chains  
205 in FPEI copolymers.

206 For the cumulative NR release test, NR-loaded FPEI micelles were incubated at three  
207 temperature points, 25, 37, and 40°C, on the basis of the results of the NR loading efficiency. **Figure**  
208 **3b** shows the temperature-dependent release behaviors of NR-loaded FPEI micelles in aqueous  
209 media as a function of the release periods. With an increase in temperature, cumulative NR release  
210 from the FPEI micelles was improved. This is because the stronger hydrophobic interactions between  
211 PPO chains and NR in the core caused the micelles to squeeze together further at higher  
212 temperatures, thereby resulting in accelerated NR release.<sup>23, 36</sup> These results also suggested that the  
213 FPEI micelles showed a potential for use in the temperature-triggered delivery of hydrophobic drugs.

214

#### 215 *3.4. Gene complexes with FPEI copolymers*

216 Having confirmed the effective loading and delivery of hydrophobic drugs in the developed  
217 nanocarriers, we next aim to co-deliver negatively-charged genetic molecules. The co-delivery of  
218 genes with drugs in the same pot has often been shown to synergize the therapeutic efficacy,  
219 including anticancer effects.<sup>37</sup> First, we sought to achieve high loading capacity of both therapeutic  
220 molecules within the nanocarrier depots, which is required for subsequent efficient release. In order to  
221 determine the DNA binding ability of FPEI, the formulation of NR-loaded FPEI complexes with pDNA  
222 was confirmed at different N/P ratios by an agarose gel retardation assay (**Figure 4a**), and their

223 surface charge was analyzed by zeta potential measurement (**Figure 4b**). These DNA complexes  
224 were electrophoresed down at an N/P ratio of 1.5, but not above an N/P ratio of 3.0. Likewise, the  
225 surface charge of the complexes increased with an increase in the N/P ratio. These results indicated  
226 that the DNA binding ability increased with an increase in N/P ratio, which was consistent with a  
227 number of typical analyses of PEI-DNA complexes.

228

### 229 *3.5. Cytotoxicity of FPEI micelles*

230 A CCK-8 assay was conducted to evaluate the *in vitro* cytotoxicity of FPEI micelles over a  
231 wide range of concentrations on HeLa cells at 37 and 40°C, as shown in **Figure 5**. After 1 h, both  
232 were incubated at 37°C for two days. FPEI samples below a concentration of approximately 250 µg/ml  
233 did not induce cytotoxicity, but those above 250 µg/ml began to show severe cytotoxicity, compared to  
234 the PF127 cytotoxicity results. A similar tendency was shown at both temperatures observed. We  
235 assumed that these results were caused by the amine groups of PEI conjugated with PF127, rather  
236 than the incubation temperature. Thus, the cytotoxicity test of PEI itself was assessed over the range  
237 of 0.5-50 µg/ml, concentration range of which was equivalent to that of PEI contained in the FPEI  
238 copolymers. The resulting PEI cytotoxicity showed a similar tendency to the results obtained for the  
239 FPEI samples. This suggested that a concentration range of FPEI micelles from the CMC up to  
240 approximately 250 µg/ml was a safe window for use in *in vitro* delivery.

241

### 242 *3.6. Temperature-dependent NR release with pGFP transfection*

243 From our preliminary experiments, the optimal N/P ratio for the best gene transfection was  
244 found at nearly 20-30 (figure not shown), and the NR concentration to make a staining difference  
245 between 37 and 40°C was approximately 10 ng/ml underlying the FPEI system. Thus, pGFP (1 µg)  
246 was added into 1 ng NR-loaded FPEI micelles (80 µg/ml) and incubated for 30 min to form stable  
247 gene complexes. The complexes were added into the HeLa cell-populated plate. At 1h after delivery,

248 a few cells with weak red fluorescence were observed in the cultures under the condition of 40°C, but  
249 not at 37°C, despite the equal exposure time (**Figure 6**). At 36 h, however, the red and green  
250 fluorescence intensity denoting NR-staining and GFP expression, respectively, became almost similar  
251 at both incubation temperatures. In comparison to these results in the presence of FPEI carriers,  
252 almost all HeLa cells exposed to free NR showed red fluorescence independently of incubation time,  
253 implying that free NR might explosively diffuse into the cytosol through the cell membrane adsorption  
254 as soon as the treatment. These results indicated that the FPEI system demonstrated a temperature-  
255 triggered NR release into the cytosol, consistent with the cumulative NR release test, along with pGFP  
256 transfection, probably following the endocytosis by PEI in the FPEI copolymers.

257

#### 258 **4. Conclusion**

259 Thermosensitive and shell cross-linked micelles composed of PF127 grafted to PEI were  
260 successfully prepared to facilitate hydrophobic drug encapsulation and formation of gene complexes.  
261 In this study, the FPEI system was logically characterized by performing sequential measurements,  
262 including the temperature-dependent size, drug loading and release behaviors, DNA binding ability,  
263 and surface charge. The FPEI system showed a potential for temperature-responsive drug release  
264 along with gene transfection in HeLa cells. Development of thermosensitive and shell cross-linked  
265 FPEI micelles suggests a promising possibility for temperature-responsive therapeutics, while further  
266 in-depth biological studies on practical therapeutic drugs and genes are needed.

267

#### 268 **Acknowledgements**

269 This work was supported by grants from the Priority Research Center Program (#2009-  
270 0093829) and Research Fellowship Program (#2013R1A1A2062694) funded by the National  
271 Research Foundation, South Korea.

272

273 **References**

- 274 1. O. Soga, C. F. van Nostrum, M. Fens, C. J. Rijcken, R. M. Schiffelers, G. Storm and W. E.  
275 Hennink, *J. Controlled Release*, 2005, **103**, 341-353.
- 276 2. D. M. Lynn, M. M. Amiji and R. Langer, *Angew. Chem. Int. Ed.*, 2001, **40**, 1707-1710.
- 277 3. E. Akar, A. Altınışık and Y. Seki, *Carbohydr. Polym.*, 2012, **90**, 1634-1641.
- 278 4. C. Katepetch and R. Rujiravanit, *Carbohydr. Polym.*, 2011, **86**, 162-170.
- 279 5. R. Cheng, F. Feng, F. Meng, C. Deng, J. Feijen and Z. Zhong, *J. Controlled Release*, 2011,  
280 **152**, 2-12.
- 281 6. K. C. Hribar, M. H. Lee, D. Lee and J. A. Burdick, *Acs Nano*, 2011, **5**, 2948-2956.
- 282 7. D. E. Meyer, B. Shin, G. Kong, M. Dewhirst and A. Chilkoti, *J. Controlled Release*, 2001, **74**,  
283 213-224.
- 284 8. T. M. Krupka, D. Dremann and A. A. Exner, *Exp. Biol. Med.*, 2009, **234**, 95-104.
- 285 9. M. Matsukata, T. Aoki, K. Sanui, N. Ogata, A. Kikuchi, Y. Sakurai and T. Okano, *Bioconjugate*  
286 *Chem.*, 1996, **7**, 96-101.
- 287 10. Y. Pan, H. Bao, N. G. Sahoo, T. Wu and L. Li, *Adv. Funct. Mater.*, 2011, **21**, 2754-2763.
- 288 11. W. Zhang, Y. Shi, Y. Chen, J. Ye, X. Sha and X. Fang, *Biomaterials*, 2011, **32**, 2894-2906.
- 289 12. A. Zintchenko, M. Ogris and E. Wagner, *Bioconjugate Chem.*, 2006, **17**, 766-772.
- 290 13. K. H. Bae, S. H. Choi, S. Y. Park, Y. Lee and T. G. Park, *Langmuir*, 2006, **22**, 6380-6384.
- 291 14. J. Y. Lee, K. H. Bae, J. S. Kim, Y. S. Nam and T. G. Park, *Biomaterials*, 2011, **32**, 8635-8644.
- 292 15. J. Sun, X. Chen, T. Lu, S. Liu, H. Tian, Z. Guo and X. Jing, *Langmuir*, 2008, **24**, 10099-10106.
- 293 16. M. Wang, B. Wu, P. Lu, C. Cloer, J. D. Tucker and Q. Lu, *Mol. Ther.*, 2013, **21**, 210-216.
- 294 17. J. Shen, Q. Yin, L. Chen, Z. Zhang and Y. Li, *Biomaterials*, 2012, **33**, 8613-8624.
- 295 18. J. I. Lee, H. S. Kim and H. S. Yoo, *Int. J. Pharm.*, 2009, **373**, 93-99.
- 296 19. E. Jeon, H. D. Kim and J. S. Kim, *J. Biomed. Mater. Res. A*, 2003, **66**, 854-859.
- 297 20. S. H. Choi, S. H. Lee and T. G. Park, *Biomacromolecules*, 2006, **7**, 1864-1870.
- 298 21. Y. Wang, L. Yu, L. Han, X. Sha and X. Fang, *Int. J. Pharm.*, 2007, **337**, 63-73.
- 299 22. S. L. Snyder and P. Z. Sobocinski, *Anal. Biochem.*, 1975, **64**, 284-288.
- 300 23. S. Seo, C.-S. Lee, Y.-S. Jung and K. Na, *Carbohydr. Polym.*, 2012, **87**, 1105-1111.
- 301 24. M. K. Gupta, T. A. Meyer, C. E. Nelson and C. L. Duvall, *J. Controlled Release*, 2012, **162**,  
302 591-598.
- 303 25. M. C. Stuart, J. C. van de Pas and J. B. Engberts, *J. Phys. Org. Chem.*, 2005, **18**, 929-934.
- 304 26. A. Convertine, C. Diab, M. Prieve, A. Paschal, A. Hoffman, P. Johnson and P. Stayton,  
305 *Biomacromolecules*, 2010, **11**, 2904-2911.
- 306 27. T. Cao, P. Munk, C. Ramireddy, Z. Tuzar and S. Webber, *Macromolecules*, 1991, **24**, 6300-  
307 6305.
- 308 28. E. Ruckenstein and R. Nagarajan, *J. Phys. Chem.*, 1981, **85**, 3010-3014.

- 309 29. M. Wilhelm, C. L. Zhao, Y. Wang, R. Xu, M. A. Winnik, J. L. Mura, G. Riess and M. D.  
310 Croucher, *Macromolecules*, 1991, **24**, 1033-1040.
- 311 30. Y. Chan, T. Wong, F. Byrne, M. Kavallaris and V. Bulmus, *Biomacromolecules*, 2008, **9**, 1826-  
312 1836.
- 313 31. Y. Li, K. Xiao, J. Luo, W. Xiao, J. S. Lee, A. M. Gonik, J. Kato, T. A. Dong and K. S. Lam,  
314 *Biomaterials*, 2011, **32**, 6633-6645.
- 315 32. J. K. Cho, W. Park and K. Na, *J. Appl. Polym. Sci.*, 2009, **113**, 2209-2216.
- 316 33. T. Delmas, A. Fraichard, P.-A. Bayle, I. Texier, M. Bardet, J. Baudry, J. Bibette and A.-C.  
317 Couffin, *J. Colloid Sci. Biotechnol.*, 2012, **1**, 16-25.
- 318 34. A.-K. Kirchherr, A. Briel and K. Ma<sup>o</sup>der, *Mol. Pharm.*, 2009, **6**, 480-491.
- 319 35. Y. Shi, M. J. van Steenberg, E. A. Teunissen, L. s. Novo, S. Gradmann, M. Baldus, C. F. van  
320 Nostrum and W. E. Hennink, *Biomacromolecules*, 2013, **14**, 1826-1837.
- 321 36. T. Y. Liu, K. H. Liu, D. M. Liu, S. Y. Chen and I. W. Chen, *Adv. Funct. Mater.*, 2009, **19**, 616-  
322 623.
- 323 37. N. Wiradharma, Y. W. Tong and Y.-Y. Yang, *Biomaterials*, 2009, **30**, 3100-3109.

324

325

326

327 **Figure captions**

328 **Figure 1.** (a) Schematic diagram showing the temperature-triggered FPEI micelle system, including  
329 its molecular structure. (b) FT-IR analysis of F127 and FPEI copolymers.

330 **Figure 2.** (a) CMC measurement of F127 and FPEI copolymers at room temperature. Arrows indicate  
331 the respective CMC. (b) Temperature-dependent size measurement of FPEI, NR-loaded FPEI, and  
332 NR-loaded FPEI complexes with DNA (n=3).

333 **Figure 3.** (a) NR loading efficiency in FPEI micelles (1, 5, and 10 mg/ml). (b) Cumulative NR release  
334 from the FPEI micelle system at 25, 37, and 40°C, based on the results of NR loading efficiency (n=3).

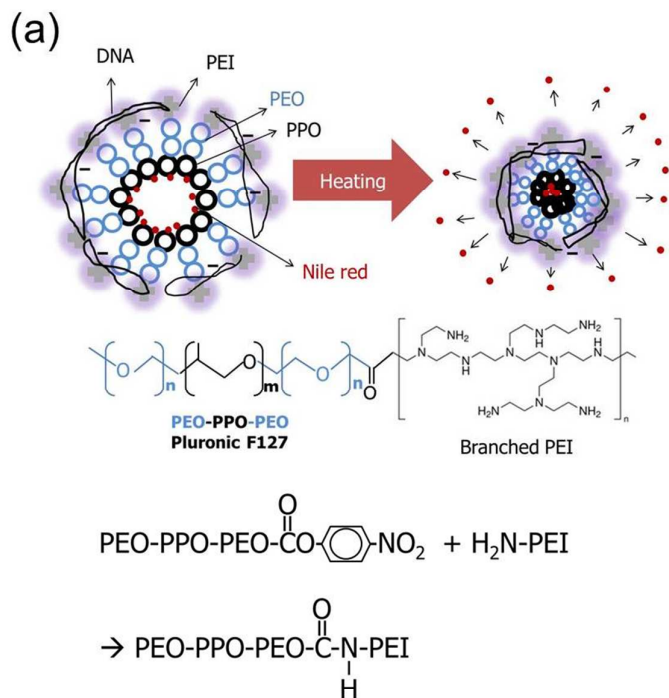
335 **Figure 4.** (a) Gel retardation assay and (b) zeta potential measurement to understand the DNA  
336 binding behavior of FPEI copolymer with an increase in N/P ratio (n=3).

337 **Figure 5.** *In vitro* cytotoxicity of F127, FPEI, and PEI, conducted on HeLa cells at 37 and 40°C.  
338 Results were presented as mean  $\pm$  SD (n=5).

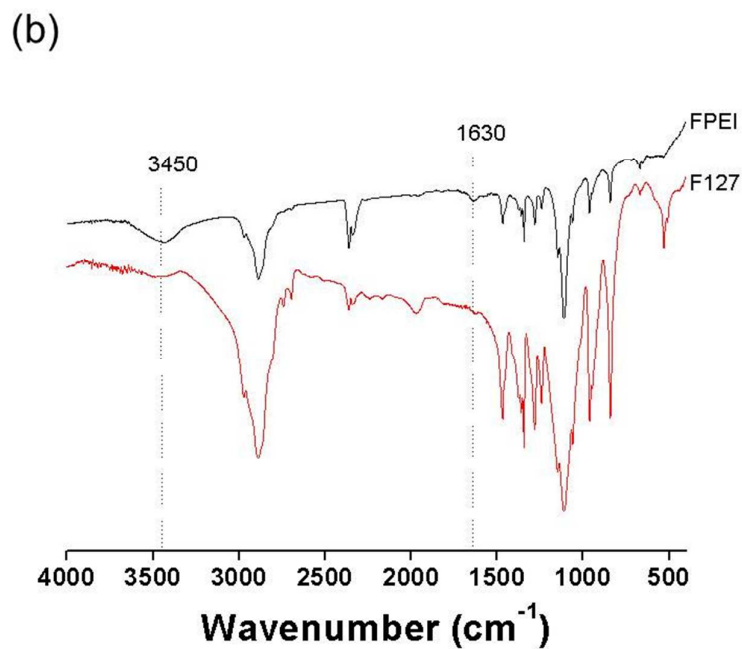
339 **Figure 6.** Fluorescence images of HeLa cells treated with GFP transfection and NR release  
340 underlying the optimized FPEI delivery system at 37 and 40°C after 1 and 36 h incubation.

341

342 Fig. 1.



343

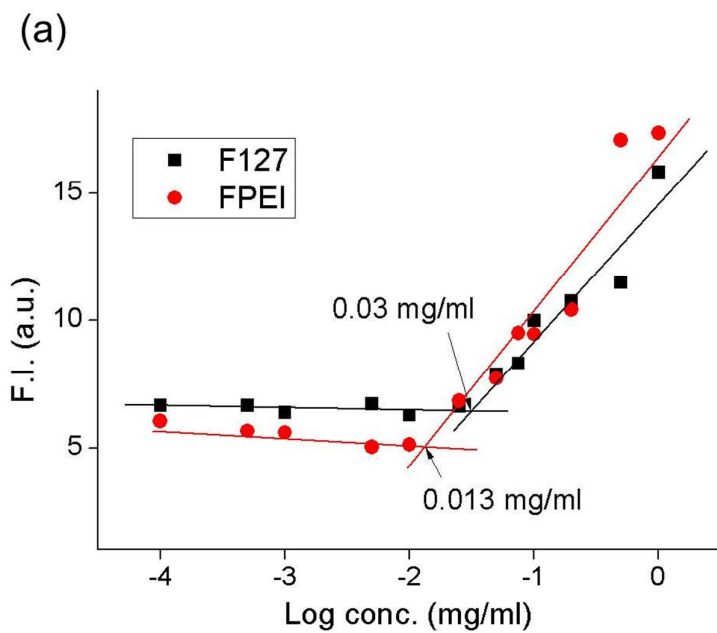


344

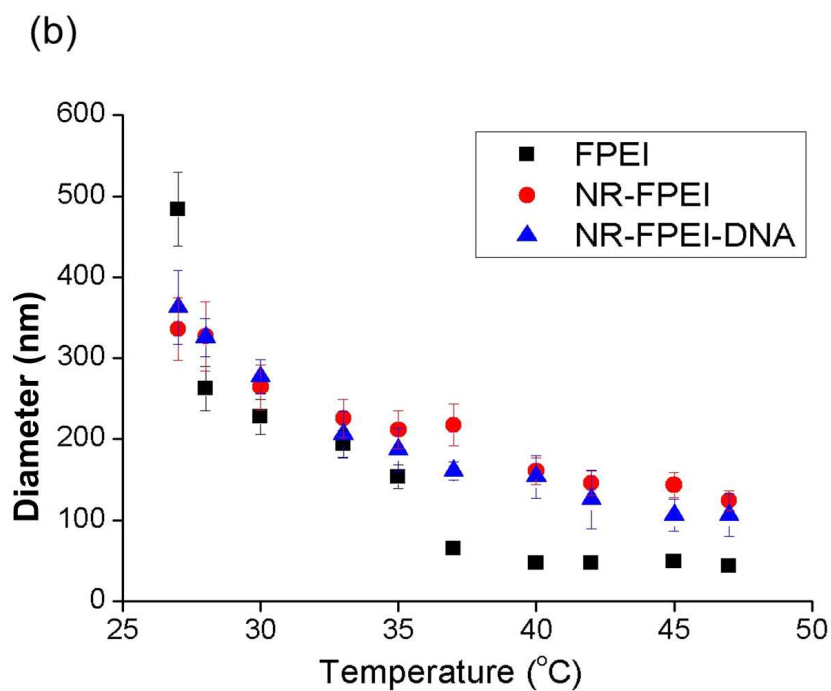
345



346 Fig. 2.



347

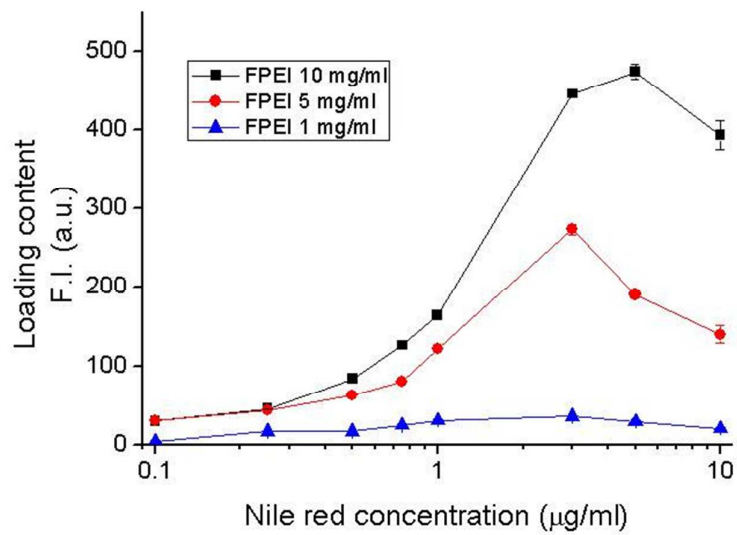


348

349

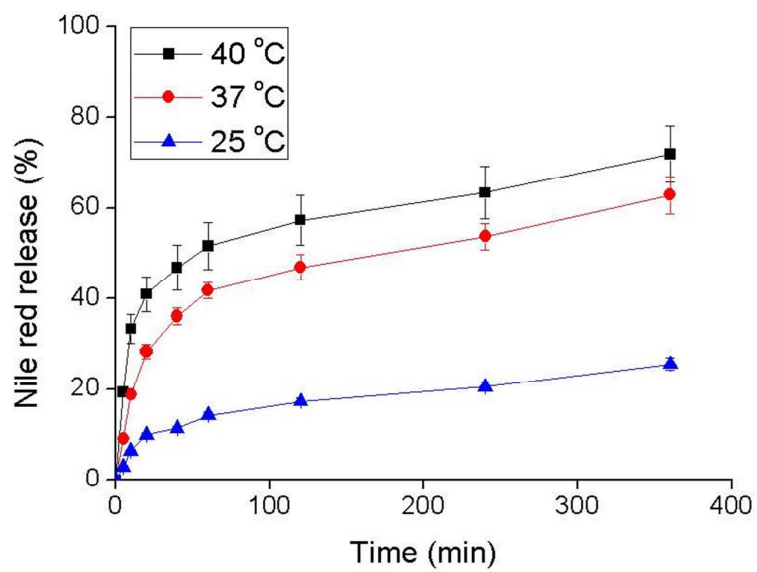
350 Fig. 3

(a)



351

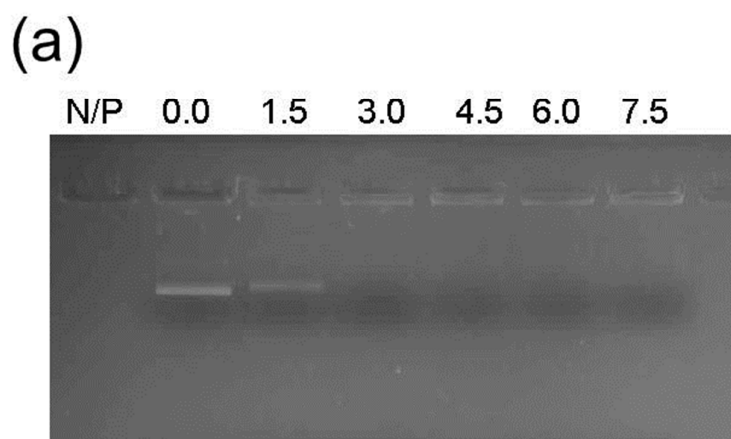
(b)



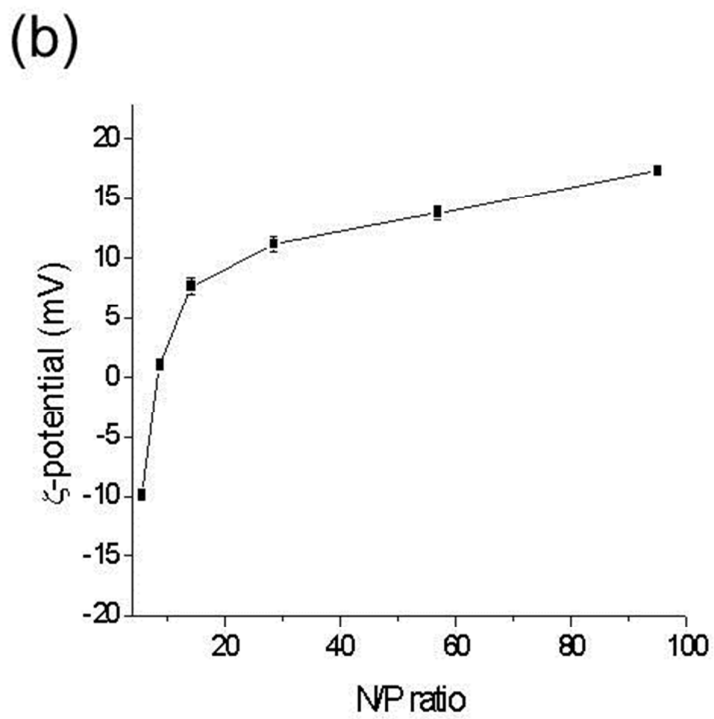
352

353

354 Fig. 4.



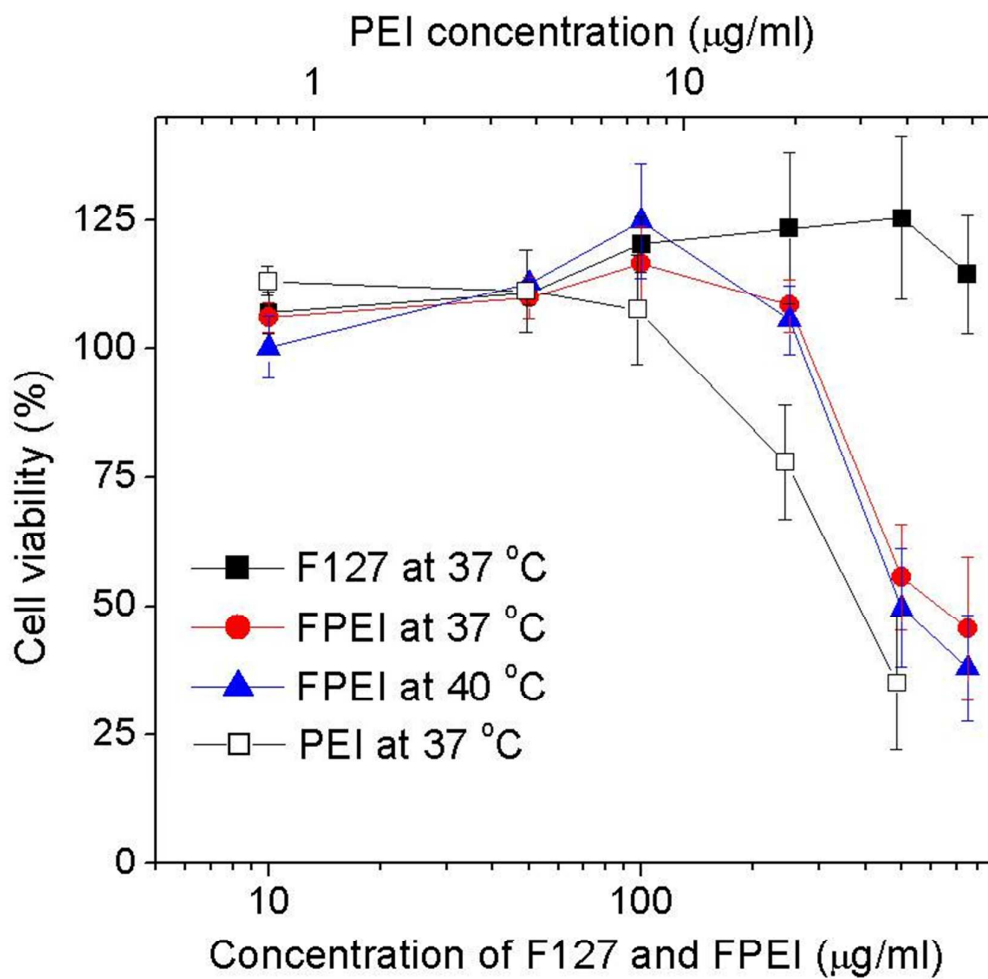
355



356

357

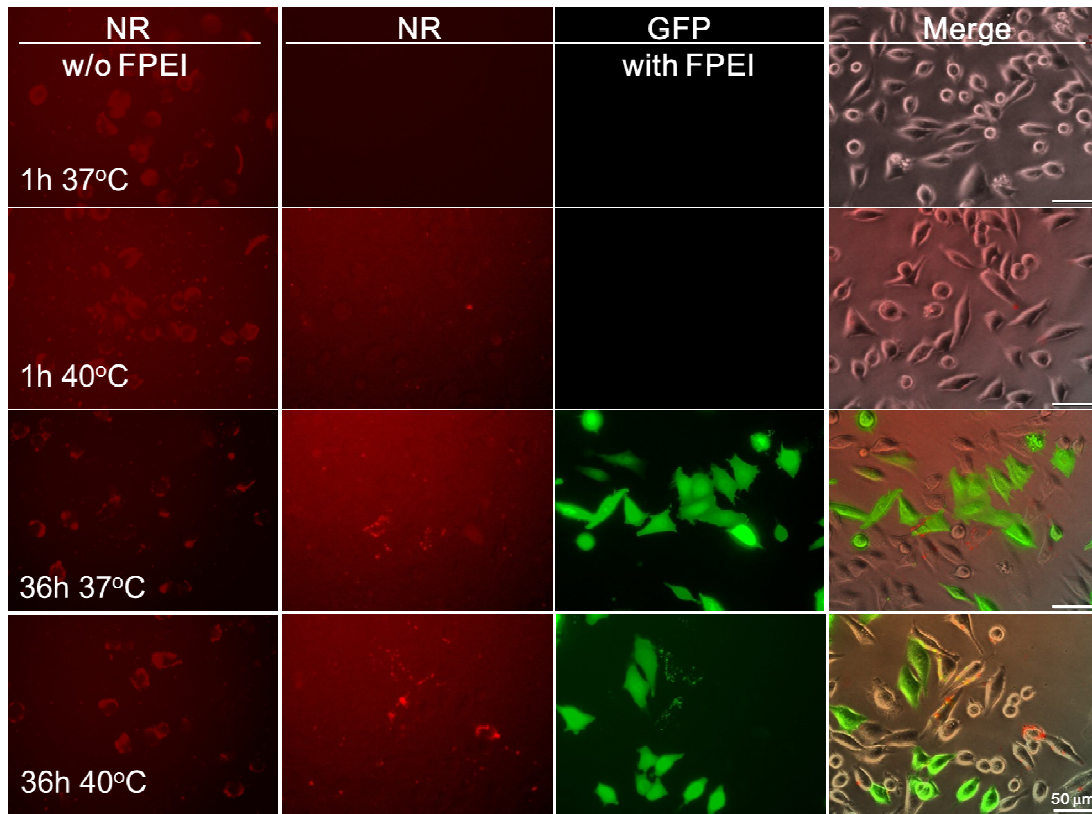
358 Fig. 5.



359

360

361 Fig. 6.



362